Inhibition of virulence-promoting disulfide bond formation enzyme DsbB is blocked by mutating residues in two distinct regions

Received for publication, December 2, 2016, and in revised form, February 9, 2017 Published, Papers in Press, February 23, 2017, DOI 10.1074/jbc.M116.770891

Cristina Landeta[1], **Brian M. Meehan**[2], **Laura McPartland, Linda Ingendahl, Feras Hatahet, Ngoc Q. Tran, Dana Boyd, and Jon Beckwith**[3]

From the Department of Microbiology and Immunobiology, Harvard Medical School, Boston, Massachusetts 02115

Edited by Ruma Banerjee

Disulfide bonds contribute to protein stability, activity, and folding in a variety of proteins, including many involved in bacterial virulence such as toxins, adhesins, flagella, and pili, among others. Therefore, inhibitors of disulfide bond formation enzymes could have profound effects on pathogen virulence. In the *Escherichia coli* disulfide bond formation pathway, the periplasmic protein DsbA introduces disulfide bonds into substrates, and then the cytoplasmic membrane protein DsbB reoxidizes DsbA's cysteines regenerating its activity. Thus, DsbB generates a protein disulfide bond *de novo* by transferring electrons to the quinone pool. We previously identified an effective pyridazinone-related inhibitor of DsbB enzymes from several Gram-negative bacteria. To map the protein residues that are important for the interaction with this inhibitor, we randomly mutagenized by error-prone PCR the *E. coli dsbB* gene and selected *dsbB* mutants that confer resistance to this drug using two approaches. We characterized *in vivo* and *in vitro* some of these mutants that map to two areas in the structure of DsbB, one located between the two first transmembrane segments where the quinone ring binds and the other located in the second periplasmic loop of DsbB, which interacts with DsbA. In addition, we show that a mutant version of a protein involved in lipopolysaccharide assembly, $lptD_{4213}$, is synthetically lethal with the deletion of *dsbB* as well as with DsbB inhibitors. This finding suggests that drugs decreasing LptD assembly may be synthetically lethal with inhibitors of the Dsb pathway, potentiating the antibiotic effects.

Protein disulfide bonds are sulfur-sulfur chemical bonds that result from an oxidative process in which two electrons are removed from a protein, linking non-adjacent cysteines of the protein. Disulfide bonds contribute to protein stability, activity, and folding (1, 2). In bacteria, proteins containing structural disulfide bonds are rarely, if at all, found in cytoplasmic compartments; they are usually present in the cell envelope or the extracellular milieu (1). Many proteins involved in bacterial virulence (such as toxins, adhesins, flagella, fimbriae, pili, and types II and III secretion systems) require disulfide bonds (3). Pathways involved in catalyzing disulfide bond formation are therefore attractive targets for identifying small molecule inhibitors, because loss of such systems can undermine the activity of numerous bacterial virulence factors as do null mutations of the genes for these enzymes (4–11).

The enzymes that promote formation of protein disulfide bonds in Gram-negative bacteria are in the cell envelope. The periplasmic enzyme DsbA, a member of the thioredoxin family, oxidizes pairs of cysteines in substrate proteins through its Cys-Xaa-Xaa-Cys active site (12). The resulting reduced DsbA is reoxidized by the cytoplasmic membrane protein DsbB, regenerating DsbA's activity (13). DsbB itself is reoxidized by membrane-embedded quinones, from which electrons are transferred to the electron transport chain (14). However, in many of the Actinobacteria and Cyanobacteria the membrane protein VKOR (vitamin K epoxide reductase) instead of DsbB is required for the reoxidization of DsbA (15). Although VKOR has no overall amino acid sequence homology with DsbB, both proteins encode two extracytoplasmic soluble domains containing essential pairs of cysteines and are capable of reoxidizing DsbA fundamentally by the same mechanism (15, 16).

We have previously generated a methodology for identifying specific inhibitors of both bacterial DsbBs and a VKOR that is based on the functional homology between the two proteins (17). The assay for inhibition of disulfide bond formation utilizes a disulfide-sensitive β-galactosidase (β-Gal^{dbs})[4] assay. This approach allowed us to identify inhibitors of either enzyme by a single high-throughput screening procedure. By this approach, we have found a family of pyridazinone-related molecules that are effective inhibitors of DsbB proteins of sev-

This work was supported in part by National Institutes of Health Grant GMO41883 from NIGMS (to J. B. and D. B.), by the Blavatnik Biomedical Accelerator at Harvard University (to J. B.), and by an industry research agreement with F. Hoffmann-La Roche Ltd. and F. Hoffmann-La Roche Inc. (to J. B.). The authors declare that they have no conflicts of interest with the contents of this article. The content is solely the responsibility of the authors and does not necessarily represent the official views of the National Institutes of Health.

This article contains supplemental Fig. S1, Schemes S1–S5, and additional information.

[1] Supported in part by a Consejo Nacional de Ciencia y Tecnología (CONACYT) postdoctoral fellowship.

[2] Supported by a Ruth L. Kirschstein National Research Service Award.

[3] To whom correspondence should be addressed. E-mail: Jon_Beckwith@hms.harvard.edu.

[4] The abbreviations used are: β-Gal^{dbs}, disulfide-bond sensitive β-galactosidase LacZ fused to the membrane protein MalF, which localizes LacZ in the periplasm making it sensitive to disulfide bond formation; MIC, minimal inhibitory concentration; P_{BAD}, arabinose promoter; $Ptrc_{204}$, promoter down mutation in −35 of pTrc99A promoter; IPTG, isopropyl β-D-1-thiogalactopyranoside.

© 2017 by The American Society for Biochemistry and Molecular Biology, Inc. Published in the U.S.A.

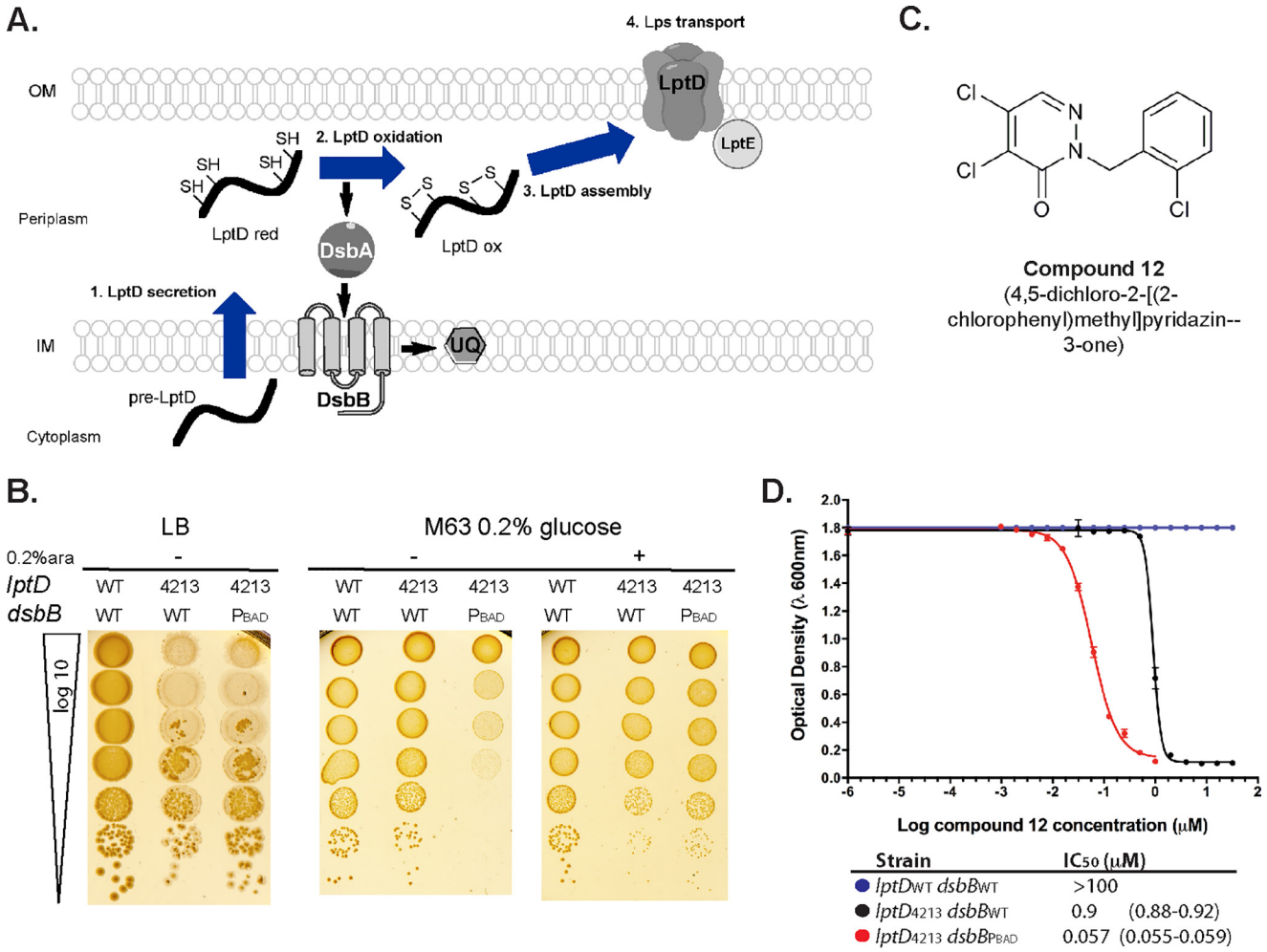

Figure 1. Synthetic lethality of *dsbB* and *lptD*$_{4213}$. *A,* disulfide bond formation and Lps transport pathways converge because LptD requires two non-consecutive disulfide bonds that are essential for LptD assembly and functioning. *Blue arrows* show the process flow of LptD secretion to assembly. *Black bold arrows* show the flow of electrons in the disulfide bond formation pathway. *SH*, thiol groups representing cysteines; *S–S*, disulfide bonded cysteines; *red,* reduced; *ox*, oxidized; *UQ*, ubiquinone; *Lps*, lipopolysaccharides; *OM*, outer membrane; *IM,* inner membrane. *B,* growth on LB-Miller and M63 agar minimal media of *lptD*$_{WT}$*dsbB*$_{WT}$ (HK295 strain), *lptD*$_{4213}$*dsbB*$_{WT}$ (CL337 strain), and *lptD*$_{4213}$Δ*dsbB dsbB*$_{PBAD}$ (CL380 strain). M63 glucose cultures with an A_{600} of 0.5 were serially diluted and spotted in the indicated agar media (10 μl). 0.2% arabinose was added to induce *dsbB* expression in CL380 strain. Plates were incubated for 2 days at 37 °C. *C,* structure of compound 12. *D,* growth on M63 minimal media broth in the presence of compound 12 of strains: HK295 (*blue circles*), CL337 (*black circles*), and CL380 (*red circles*). Values represent the average of at least three independent experiments with 95% confidence intervals in parentheses.

eral Gram-negative bacteria but do not inhibit a bacterial VKOR.

Because we have sought to develop DsbB inhibitors as antivirulents/antibiotics, we wanted to understand how resistance to these compounds might arise *in vivo* as well as how pyridazinones inhibit DsbB. To this end, we report here mutants of DsbB that confer resistance to that inhibition. We used two methods for direct selection of spontaneous mutants of DsbB resistant to one of the strongest pyridazinone inhibitors. These selections have failed to yield any mutants that have altered DsbB. However, when we randomly mutagenize by error-prone PCR a *dsbB* gene, which is carried on a high copy number plasmid, DsbB mutants resistant to our inhibitors can be isolated. Characterization of these DsbB mutant proteins shows that they all exhibit lower affinity toward ubiquinone and menadione, and two of them show higher turnover numbers. Our studies suggest that resistance of DsbB to pyridazinone inhibitors is difficult to obtain by spontaneous selections perhaps due to the effects of inhibitor-resistant mutations on the normal functioning of DsbB. The location within the DsbB protein of the amino acid changes that do confer resistance provides suggestions as to the mechanism of inhibition and regions of the protein that influence quinone binding.

Results

Selection of mutations that confer resistance to compound 12, a pyridazinone inhibitor of DsbB

We have developed a genetic selection for mutants resistant to inhibitors of DsbB that uses an *Escherichia coli* strain further sensitized to the inhibitor by the presence of an additional mutation (*lptD*$_{4213}$). In Gram-negative bacteria, a set of *lpt* genes encodes proteins required for the transport and assembly of lipopolysaccharides (LPS) into the outer leaflet of the outer membrane. The Lpt proteins are essential for *E. coli* growth. LptD is an outer membrane β-barrel protein, which requires two disulfide bonds for its proper assembly and function, and it is involved in the last steps of LPS assembly (Fig. 1*A*) (18).

Despite the essentiality of LptD, strains lacking a functional disulfide bond formation pathway remain viable under aerobic conditions presumably because background oxidation can lead to sufficient spontaneous disulfide bond formation in LptD and other essential proteins (19). We considered the possibility that a strain carrying the $lptD_{4213}$ mutant allele ($LptD_{4213}$) (20) might be hypersensitive to a loss of DsbA or DsbB. This mutant LptD, which lacks residues 330–352, displays major defects in protein maturation and assembly, and strains carrying such an allele show increased membrane permeability to detergents, bile salts, and antibiotics (21–24). In such a compromised strain, the loss of the disulfide bond machinery might be lethal.

As a first step in testing for this potential synthetic lethality, we introduced a plasmid with a regulatable copy of *dsbB* cloned under the arabinose promoter (pCL67) into a $dsbB^+$ strain encoding the $lptD_{4213}$ allele (CL337 strain). We then attempted to transduce a deletion of the genomic copy of *dsbB* into the $lptD_{4213}$ strain. Although Δ*dsbB* transductants were readily obtained when a second copy of *dsbB* was present, we were not able to isolate transductants in the strain encoding only one copy of *dsbB* unless cystine was added to the medium, which yielded a lower frequency than having two *dsbB* copies. Cystine is an oxidant that can mediate disulfide bond formation in the absence of the disulfide bond formation pathway (13). Furthermore, the strain carrying the plasmid with *dsbB* under an arabinose promoter ($lptD_{4213}$Δ*dsbB* $dsbB_{PBAD}$, CL380 strain) was able to grow on LB, although it did not grow on minimal media unless 0.2% arabinose was added (Fig. 1*B*). Thus, *dsbB* and $lptD_{4213}$ are a synthetically lethal combination.

We then asked whether the $lptD_{4213}$ mutant strain was sensitive to a particularly potent *E. coli* DsbB inhibitor, compound 12 (4,5-dichloro-2-[2-chlorophenyl]methylpiridazin-3-one, Fig. 1*C*). We have shown that compound 12 forms a covalent bond with the second cysteine of DsbB (Cys-44) (17). Ordinarily, quinones, the direct source of oxidation of DsbB, form a charge-transfer complex with Cys-44 of DsbB during the process of electron transfer between DsbA and DsbB (25). We have proposed that the inhibition of DsbB activity by pyridazinone compounds, including compound 12, results from the competition with quinone for the quinone-binding site leading to the covalent reaction with Cys-44, thus inactivating the protein (17). We observed that, unlike the strain with wild type *lptD*, the $lptD_{4213}$ strain was highly sensitive to compound 12 as demonstrated by the inhibition of growth in a concentration-dependent manner (*black circles,* Fig. 1*D*). Because we have demonstrated that compound 12 targets DsbB (by interfering with DsbA reduction, exhibits a decrease in motility and an increase in the disulfide bond-sensitive β-galactosidase) (17), these data also indicated that the combination of the $lptD_{4213}$ and *dsbB* inhibition results in a synthetic lethal interaction. In addition, the conditionally lethal strain $lptD_{4213}$Δ*dsbB* $dsbB_{PBAD}$ was even more sensitive to compound 12 when no arabinose was present in liquid minimal media where disulfide bond formation is partly dependent on air oxidation (*red circles,* Fig. 1*D*).

The findings above suggested that selecting for growth of a strain that contains the $lptD_{4213}$ allele and is exposed to the DsbB inhibitor, compound 12, could yield inhibitor-resistant mutants. We therefore plated the $lptD_{4213}$ strain on M63 minimal media with 10 μM compound 12, a concentration of drug ~10-fold higher than the minimal inhibitory concentration (MIC). Although mutants were obtained at a very low frequency ($\sim 10^{-8}$) when exposed to the compound, none of them mapped to the *dsbB* gene but rather to the gene *bamB*. Twenty two of 51 colonies analyzed by PCR yielded a larger than expected product for the *bamB* region, and the sequence of all these indicated an insertion of an IS1 element in the gene. Whole-genome sequencing was performed in three of the colonies in which the *bamB* product was similar in size to wild type. Two of these encoded mutations within *bamB* ($BamB_{E240*}$ and $BamB_{\Delta 252-255}$). Both mutations, *bamB*::IS1 and $BamB_{\Delta 252-255}$, are known to be loss of function mutants of BamB that confer similar phenotypes (22). Therefore, these mutations most likely inactivated the outer membrane lipoprotein BamB, a scenario known to bypass the assembly defect of $LptD_{4213}$ (22, 26–28).

Selection of mutations that confer resistance to compound 12 by PCR mutagenesis of the dsbB gene

Because our initial selection for *dsbB* mutants resistant to compound 12 did not yield any mutations in that gene, we decided to use the same $LptD_{4213}$ strain to select for mutants resistant to compound 12 using a randomly mutagenized *dsbB* library. To do this, we mutagenized *dsbB* via error-prone PCR and cloned the resultant PCR products into a plasmid in which *dsbB* expression is under the control of an IPTG-inducible promoter. This pool of plasmids was then transformed into the conditionally lethal strain $lptD_{4213}$Δ*dsbB* $dsbB_{PBAD}$ selecting for the presence of the plasmid using the antibiotic marker. The transformation yielded ~4,500 independent colonies carrying both a plasmid with an arabinose-inducible wild type *dsbB* and a plasmid with an IPTG-inducible mutated *dsbB.* The colonies were scraped up, pooled together, and plated on selection plates of M63 glucose with 10 μM compound 12, which is ~10-fold higher than the MIC observed for the strain carrying the two plasmids expressing wild type *dsbB*. Because glucose represses transcription of wild type *dsbB* from the P_{BAD} promoter, these conditions select for resistant DsbBs expressed from the mutant library. We obtained 20 colonies and sequenced only the mutagenized *dsbB* gene from the IPTG-inducible plasmid (see "Materials and methods"). We found that 9 of 20 colonies (45%) had mutations in DsbB (Fig. 2*A*) and 6 of these 9 colonies encoded a change of Leu-25 to Pro in combination with a second mutation in residues Gln-134 or Glu-141, both located in the periplasmic loop that interacts with DsbA (Phe-64–Gly-65) just after Cys-130, which attacks the disulfide of Cys-41–Cys-44 of DsbB (29). However, 11 of 20 colonies (55%) did not have mutations in the mutagenized *dsbB* gene, and 5 of these 11 encoded mutations in the *trc* promoter region, possibly leading to increased DsbB expression.

Anaerobic selection of mutations that confer resistance to compound 12

The Dsb pathway is not essential for aerobic growth of *E. coli*. However, under anaerobic conditions, *dsbA* and *dsbB* mutants

A.

AEROBIC SELECTION

Nucleotide change	Amino acid change	Number of isolates
Non-synonymous substitution		
T77C/A425G	L25P/E141G	4
T77C/A404G	L25P/Q134R	2
T218C	V72A	1
T235G	L78V	1
C506T	A168V	1
Mutations elsewhere *dsbB*		
In *Trc* promoter (WT *dsbB*)	-	5
WT sequence	-	6

ANAEROBIC SELECTION

Nucleotide change	Amino acid change	Number of isolates
Non-synonymous substitution		
G26A	C8Y	2
T50A	L16Q	6
T77C	L25P	27
C89T	A29V	1
A118G	K39E	5
C301T	P100S	2
A310G	T103A	5
T319C	F106L	3
T320A	F106Y	2
C430T	P143S	1
Synonymous substitution		
C10A	-	1
G51A	-	8
G51T	-	11
T112C	-	1
T216C, T267C	-	1
Mutations elsewhere *dsbB*		
WT sequence	-	6

B.

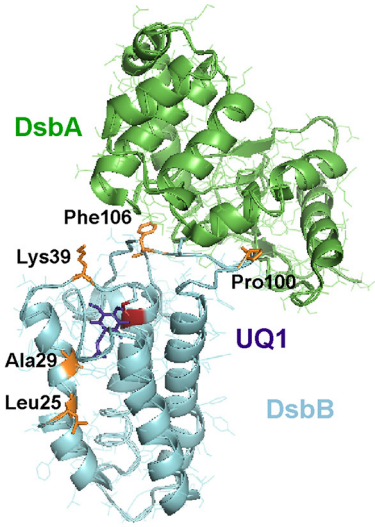

C.

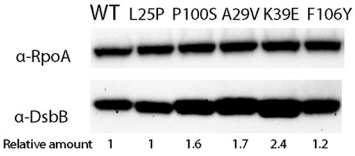

Figure 2. Compound 12-resistant mutations using two different selections. *A,* nucleotide changes found in *dsbB* after selection of $LptD_{4213}$ growth on aerobic minimal media in the presence of 10 μM compound 12 (*top*). Nucleotide changes found in *dsbB* after selection on anaerobic minimal media in the presence of 2 μM compound 12 (*bottom*). The mutations studied in this work are indicated with an *orange circle*. *B,* location of the mutations (*orange*) in the structure of the DsbA-DsbB complex. DsbA is shown in *green*, DsbB in *cyan*, Cys-44 in *red,* and ubiquinone-1 (*UQ1*) in *purple*. PyMOL was used to visualize the structure (2ZUP) of the crystallized complex when Cys-30 of DsbA is forming a disulfide bond with Cys-104 of DsbB and Cys-41 and Cys-44 of DsbB are disulfide bonded. *C,* α-DsbB immunoblot analysis of strains carrying *dsbB* at λ *att* site under the control of trc_{204} promoter (CL591 to CL596 strains). Cells were grown for 4 h in M63 minimal medium with 0.2% glucose and 1 mM IPTG to induce expression of DsbB. Cells were TCA-precipitated, and protein pellets were resuspended in 100 mM Tris, 1% SDS buffer. β-Mercaptoethanol was used to reduce the proteins. 10 μg of total protein samples were loaded in 12% acrylamide gel. α-RpoA was used as a loading control. The relative amount was calculated using arbitrary levels given by Image Lab 5.2 software.

do not grow.[5] Compound 12 inhibits anaerobic growth of an *E. coli* wild type strain at 1 μM (17). We therefore sought to isolate mutants resistant to this inhibitor using a selection for anaerobic growth in the presence of 2 μM compound 12. We again observed that spontaneous resistant mutations arose at a very low frequency ($\sim 10^{-7}$), and none of them mapped to the *dsbB* gene.[5] However, whole-genome sequencing of four of these resistant mutants indicated that all of them encoded mutations in the gene encoding thioredoxin reductase ($TrxB_{P16L}$, $TrxB_{D287Y}$, $TrxB_{S143F}$, and $TrxB_{\Delta 231-236,\ V237I}$). TrxB is a critical component in the disulfide bond isomerization pathway, and mutations in this pathway have been shown to partially restore disulfide bond formation (30).

We again made use of the same library of plasmids containing the PCR-mutagenized *dsbB* and transformed them into an *E. coli* Δ*dsbB* strain, selecting aerobically for the presence of the plasmid using the antibiotic marker. The transformation yielded ~3,000 independent colonies. This mutant pool was plated anaerobically on solid media containing M63 glucose with 40 mM fumarate, 2 μM compound 12 and solidified with 1% agarose. This concentration of compound 12 is twice the MIC normally seen under these conditions. From this selection, we isolated 82 resistant colonies and sequenced the *dsbB* gene of each (Fig. 2*A*). Most (92%) encoded mutant *dsbB* alleles. The most frequently isolated mutation was $DsbB_{L25P}$ similar to our $lptD_{4213}$ selection, which could indicate a mutational hot spot that caused enrichment for this mutant in our library or a more effective resistance.

Characterization of five DsbB mutants

We observed that the mutations encoding resistance to compound 12 localized to two regions in the structure of DsbB, the quinone-binding site in the region of the first two transmembrane helices of DsbB and a segment of the periplasmic loop of the protein that interacts with DsbA during DsbA-DsbB complex formation (Fig. 2*B*).

We selected five of the mutants to study further (Fig. 3*A*) as follows: L25P (which was found in two different selections), A29V, K39E, P100S, and F106L, which included alterations of the two distinct regions, *i.e.* near the cysteines that bind to quinone and near the cysteines that bind to DsbA located in the periplasmic loop. We assessed the DsbB levels in the mutants to verify that the resistance to the drug was not due to an increased amount of DsbB. Four of the five mutants showed no difference in the amount of DsbB expression when 1 mM IPTG is added (Fig. 2*C*). The K39E mutant exhibited a 2-fold increase in DsbB levels for reasons that are not clear.

To gain insights into the resistance displayed by DsbB mutants, we purified the proteins and analyzed their enzyme kinetics using an ubiquinone reduction assay (31). We observed that although the affinity toward ubiquinone (K_m) of the wild

[5] B. M. Meehan. C. Landeta, D. Boyd, and J. Beckwith, manuscript in preparation.

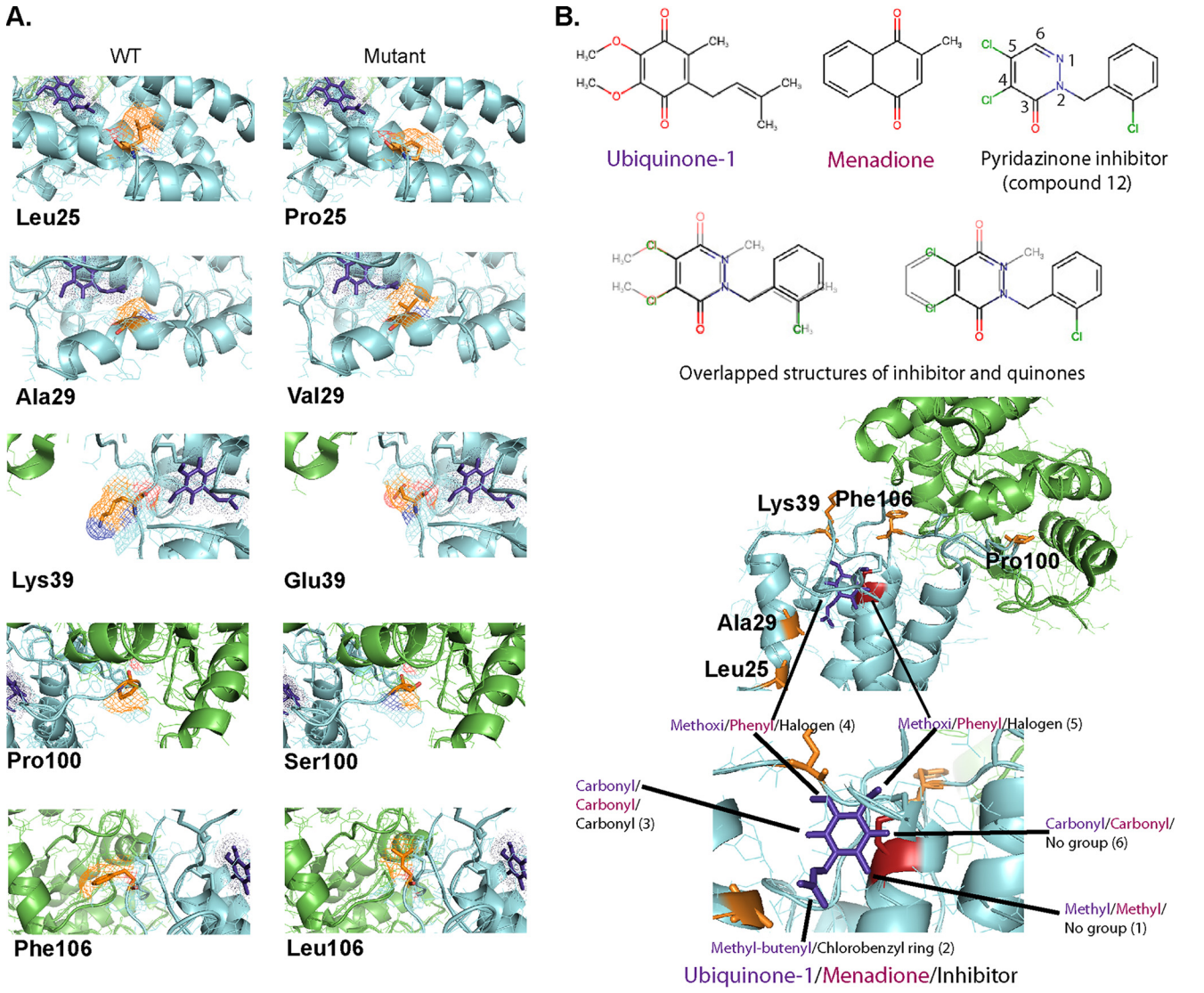

Figure 3. Visualization of mutations in DsbB structure and binding prediction of pyridazinone inhibitors (compound 12). *A,* comparison of mutated residues in the structure of DsbB and in relation to ubiquinone. *B,* overlap of ubiquinone or menadione and compound 12 in the structure of DsbB. Residues studied in this work are highlighted in *orange*, DsbA in *green*, DsbB in *cyan*, Cys-44 in *red,* and ubiquinone-1 in *purple*. PyMOL was used to visualize the structure (2ZUP) of the crystallized complex.

type enzyme is 0.9 μM, the affinity of all five mutants exhibited 2–10-fold higher K_m values (Table 1, 4th column), suggesting that the mutations directly impacted the binding of the ubiquinone substrate. Only $DsbB_{K39E}$ and $DsbB_{F106L}$ mutants showed 2-fold higher turnover rates (k_{cat}) than the wild type enzyme (Table 1, 2nd column). We also tested DsbB mutants in a menadione (vitamin K3) reduction assay because menaquinones are used primarily during anaerobic growth (14). Similarly to ubiquinone, all mutants displayed higher K_m values for menadione, with the greatest increases observed in $DsbB_{L25P}$, $DsbB_{A29V}$, and $DsbB_{K39E}$ (about 2–5-fold increases; Table 1, 5th column). In terms of turnover rate using menadione (Table 1, 3rd column), mutants $DsbB_{L25P}$, $DsbB_{P100S}$, and $DsbB_{F106L}$ displayed about one-third of the wild type rate, whereas $DsbB_{K39E}$ shows a 2-fold lower rate than wild type enzyme. Overall, the catalytic efficiency (k_{cat}/K_m) of the mutants was lower than wild type (Table 1, 6th and 7th columns).

We also measured the inhibition of DsbB by compound 12 using an *in vitro* assay with purified components in the ubiquinone reduction assay (Table 1, 8th column). $DsbB_{A29V}$ displayed a 50-fold increase in the IC_{50}, whereas $DsbB_{L25P}$ and $DsbB_{K39E}$ showed a 5- and 2-fold increase, respectively, under saturating concentrations of ubiquinone and DsbA. Under these conditions, neither $DsbB_{P100S}$ nor $DsbB_{F106L}$ showed an increase in the IC_{50} (see under "Discussion").

Mutations isolated anaerobically conferred resistance aerobically to $LptD_{4213}$ strain

We then asked whether the DsbB mutants obtained in the anaerobic selection also conferred resistance when tested in our aerobic model using the $LptD_{4213}$ strain. We transformed the IPTG-inducible *dsbB* mutant plasmids obtained anaerobically into the $lptD_{4213}\Delta dsbB$ strain carrying a plasmid with an arabinose-inducible wild type *dsbB*. We then determined

Table 1

***In vitro* and *in vivo* properties of DsbB mutants**

Values represent the average of at least two independent experiments ± S.E. or the 95% confidence intervals in parentheses.

Mutant	k_{cat}[a]		K_m[b]		k_{cat}/K_m		IC_{50} of compound 12	
	Ubiquinone	Menadione	Ubiquinone	Menadione	Ubiquinone	Menadione	*In vitro*[c]	*In vivo*[d]
	μM						μM	
$DsbB_{WT}$	2.8 ± 0.07	1.9 ± 0.05	0.94 ± 0.1	35.8 ± 2.8	2.99	5.3×10^{-2}	0.033 (0.029–0.039)	1.14 (1.09–1.18)
$DsbB_{L25P}$	2 ± 0.03	0.54 ± 0.05	2.3 ± 0.1	174 ± 25	0.88	0.31×10^{-2}	0.173 (0.157–0.192)	4.06 (3.84–5.52)
$DsbB_{A29V}$	3 ± 0.2	1.4 ± 0.05	10.8 ± 1.5	90.5 ± 6.5	0.28	1.5×10^{-2}	1.697 (1.54–1.79)	1.47 (1.39–1.56)
$DsbB_{K39E}$	5.5 ± 0.2	0.8 ± 0.1	3 ± 0.4	201 ± 38	1.81	0.39×10^{-2}	0.071 (0.065–0.079)	3.01 (2.75–3.30)
$DsbB_{P100S}$	2.1 ± 0.06	0.66 ± 0.03	3.6 ± 0.4	47 ± 5.1	0.58	1.4×10^{-2}	0.033 (0.030–0.037)	2.01 (1.93–2.1)
$DsbB_{F106L}$	6.2 ± 0.09	0.69 ± 0.08	3.6 ± 0.2	61.8 ± 15	1.73	1.1×10^{-2}	0.055 (0.049–0.063)	1.2 (1.05–1.37)

[a] k_{cat} expressed as nanomoles of ubiquinone-1 or menadione per nmol of DsbB per s.
[b] K_m values represent ubiquinone-1 or menadione concentrations.
[c] *In vitro* inhibition was measured using 10 nM DsbB, 10 μM ubiquinone-1, and 20 μM reduced DsbA.
[d] *In vivo* inhibition was measured by growth inhibition of strain $lptD_{4213}\Delta dsbB\ dsbB_{Ptrc204}$ (CL409–410, CL416–417, and LI18–19 strains) in the presence of drugs.

whether these mutants were able to support growth of $lptD_{4213}\Delta dsbB$ strain by curing the plasmid encoding the arabinose-inducible wild type *dsbB* (see "Materials and methods"). All DsbB mutants were able to support growth of $lptD_{4213}\Delta dsbB$ strain indicating that the mutants selected anaerobically are also functional aerobically. These strains were then tested for growth in the presence or absence of compound 12 in minimal medium. The results are shown in Table 1 (9th column). $DsbB_{L25P}$ and $DsbB_{K39E}$ exhibited a 3–4-fold increase in the IC_{50}, whereas the $DsbB_{P100S}$ mutant showed a modest increase. Hence, these mutants isolated anaerobically can also confer resistance to compound 12 aerobically. In contrast, $DsbB_{A29V}$ and $DsbB_{F106L}$ mutants did not show a significant increase of the IC_{50} under these conditions (see "Discussion").

Compound 12-resistant mutants are also resistant to other pyridazinone analogs

We have previously performed structure/activity analysis with pyridazinones and found compound 12 to be one of the most effective inhibitors (17). Here, we explored other variations in the structure of the molecule in the hope of finding more effective compounds as well as gaining insight into the mechanism of action of this class of drugs. The results of this analysis are shown in Table 2 and described under "Materials and methods." We found compound 36 more effective than compound 12, and compounds 37 and 38 were as effective as compound 12 in our β-galactosidase assay. Our results showed that changing both halogens (electron acceptors) in the pyridazinone ring to methyl groups (electron donors) makes the drug ineffective; similarly, changing the halogen at position 5 to methyl (Table 2, see Fig. 3*B* for atom numbers) while changing the halogen at position 4 to methyl only decreases the inhibitor efficacy (Table 2), thus suggesting that the halogen at position 5 is the leaving group in the covalent interaction with Cys-44 of DsbB. To confirm this possibility, we analyzed the inhibition of DsbB by mass spectrometry. When compounds 12 or 38 are incubated with the DsbB-$DsbA_{C33A}$ complex, a mass decrease of 36.7 and 36.8 Da, respectively, is observed indicating a loss of a chloride (plus a proton) (Table 3). Although with compounds 36 or 37, the measured molecular mass of the complex compound is decreased by 80.9 and 81.4 Da, respectively, indicating a loss of a bromide (plus a proton) (Table 3). These data provide evidence that the halogen at position 5 of the pyridazinone ring is the leaving group when covalently binding to Cys-44 of DsbB.

We determined whether the residues important for resistance to compound 12 also led to resistance in other strong inhibitors of the pyridazinone family. We tested the five DsbB mutants *in vivo* using the $LtpD_{4213}$ strain and found that, like compound 12, all are resistant to the other pyridazinone inhibitors. $DsbB_{L25P}$ and $DsbB_{K39E}$ showed 2–5-fold increases in the IC_{50} for all of the pyridazinone inhibitors (Table 4). In addition, $DsbB_{A29V}$, $DsbB_{P100S}$, and $DsbB_{F106L}$ showed an almost 2-fold increase in the IC_{50} for at least two of the inhibitors tested (Table 4). Thus, we observed at least some level of cross-resistance to pyridazinones for all DsbB mutants.

Discussion

In the oxidation pathway that introduces disulfide bonds into proteins in the bacterial periplasm, DsbA cysteines need to be reoxidized to start a new catalytic cycle. The cytoplasmic membrane protein DsbB performs this task. DsbB is a cellular machine that generates a protein disulfide bond *de novo* at the expense of electrons to be transferred to ubiquinone (14, 32). During the transfer and interaction of DsbA with DsbB, the latter undergoes conformational changes (29). In this work, we have selected DsbB mutants that confer resistance to a pyridazinone inhibitor and are located in two prominent areas in the structure of DsbB, one located between the two first transmembrane segments where the quinone ring fits. These mutants, $DsbB_{L25P}$, $DsbB_{A29V}$, and $DsbB_{K39E}$, show a higher K_m value for quinones as one might expect given that they are in the region of the quinone binding (Fig. 2*B*). Surprisingly, the other area is located in the second periplasmic loop of DsbB known to interact with DsbA. It has been shown that this segment from Pro-100 to Phe-106 is accommodated deep in the hydrophobic groove of DsbA's structure (29, 33). The fact that we find mutants in this region and that $DsbB_{P100S}$ and $DsbB_{F106L}$ mutants exhibit an increase in the K_m value for quinone despite not being located within the quinone-binding site suggests that this region also shapes the DsbB-quinone interaction. This model is in agreement with the fact that this segment of DsbB has to be mobile because it contains the Cys-104 residue that forms a disulfide with Cys-30 of DsbA and participates in the exchange of disulfides with Cys-41–Cys-44 of DsbB to finally oxidize DsbA (34).

Levels of DsbB were assessed in the mutants to demonstrate that the resistance to compound 12 is not due to changes in DsbB amount (Fig. 2*C*). Although levels remained unchanged

TABLE 2
Relative inhibition of DsbB by other pyridazinone drugs

ID Number	Structure	Inhibition Ratio (RIC_{50} Compound 12/RIC_{50} Compound)*
36 (G1-4)	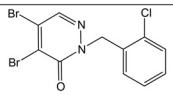	6.4
12	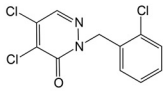	**1**
37 (G1-7)	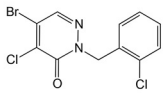	0.55
38 (G1-3)	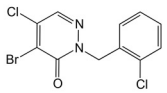	0.5
39 (G3-4)	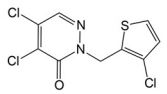	0.11
40 (G2-1)	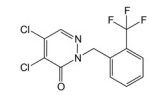	0.05
41 (G2-2)	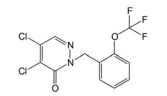	0.022
42 (G1-1)	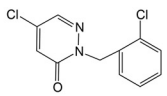	0.019
43 (G3-2)	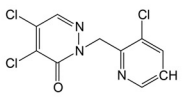	0.015
44 (G3-1)	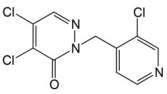	0.011
45 (G1-2)	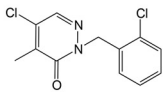	0.008
46 (G3-3)	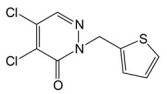	0.005
47 (G2-3)	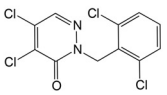	0.00002

* The RIC_{50} values were obtained using β-galactosidase activity, which is a measure of the inhibition of DsbB in *E. coli* expressing β-Gal^{dbs}. The more DsbB inhibition of a drug the more β-galactosidase activity will be observed in cells, so one can calculate the concentration that gives 50% of inhibition (RIC_{50}) of the total activity observed in a Δ*dsbB* strain and use that concentration to get the fold-increase by dividing the RIC_{50} of compound 12 (0.16 μM, 95% confidence interval 0.13–0.20 μM) between the RIC_{50} of the tested drug. Thus, a drug more potent than compound 12 will have a higher ratio and vice versa. The results were obtained using data of at least three independent experiments.

TABLE 2—*continued*

ID Number	Structure	Inhibition Ratio (RIC_{50} Compound 12/RIC_{50} Compound)*
48 (G1-6)	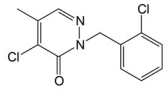	<<0.00001
49 (G1-8)	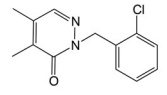	<<0.00001
50 (G1-10)	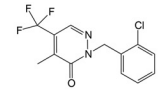	<<0.00001
51 (G1-5)	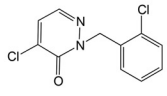	<<0.00001
52 (G1-11)	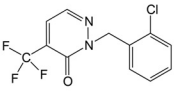	<<0.00001
53 (G1-12)	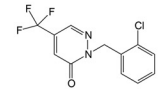	<<0.00001
54 (G1-9)	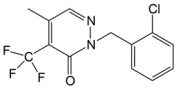	<<0.00001
55 (G2-4)	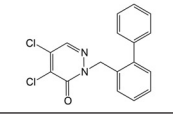	<<0.00001

TABLE 3
Summary of deconvoluted masses obtained from ESI-MS analysis of non-reduced proteins treated with compounds

Compound	Structure	Compound's MW (Da)	Measured MW of DsbB-$DsbA_{C33A}$ complex	Mass increase upon incubation with compound (Da)	Mass loss (Da)
No compound	-	-	43184.3 ± 3.2	-	-
12	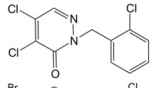	289.5	43437.1 ± 1.7	252.8	36.7
36	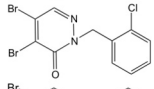	378.44	43481.8 ± 2.2	297.5	80.9
37	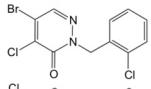	333.99	43437.0 ± 2.0	252.6	81.4
38	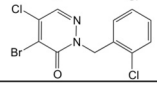	333.99	43481.5 ± 2.3	297.2	36.8

in four of the five mutants, due to unknown reasons $DsbB_{K39E}$ showed a 2-fold increase in DsbB. Although we cannot rule out the possibility that the increase in DsbB levels may contribute to the resistance of $DsbB_{K39E}$, the purified mutant displayed significantly different kinetics than the wild type enzyme, suggesting that the resistance conferred by the mutation is at least partially due to its effects on enzyme activity. This study highlights the decrease in quinone affinity rendering the mutants less susceptible to inhibition. The mutations may selectively inhibit access of the compound to Cys-44 while allowing limited passage of quinone. However, two mutants $DsbB_{K39E}$ and $DsbB_{F106L}$ also show an increase in k_{cat} implying that the reac-

TABLE 4

DsbB mutants give *in vivo* resistance against pyridazinone-related molecules

Values represent the average of three independent experiments with the 95% confidence intervals in parenthesis. Boldface numbers have more than a 2-fold increase compared with wild type. Underlined numbers have 1.8–1.9-fold increase of IC_{50}. Values that do not have a 95% confidence interval is due to the lack of higher concentrations tested given the poor solubility of some compounds in minimal media.

ID	Structure	*In vivo* IC_{50}[+]					
		DsbB	DsbB L25P	DsbB A29V	DsbB K39E	DsbB P100S	DsbB F106L
36	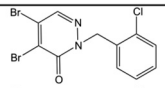	0.31 (0.25-0.39)	**0.98** (0.94-1.02)	0.45 (0.35-0.56)	**0.91** (0.83-0.99)	0.42 (0.4-0.44)	0.3 (0.19-0.46)
37	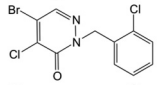	0.61 (0.58-0.64)	**1.35** (1.3-1.4)	0.52 (0.47-0.57)	**2.34** (2.08-2.64)	**1.18** (1.16-1.2)	0.5 (0.37-0.68)
38	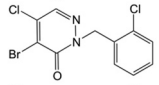	0.42 (0.39-0.45)	**2.2** (2.13-2.28)	**1.29** (1.24-1.33)	**1.31** (1.24-1.37)	0.52 (0.45-0.61)	**0.8** (0.76-0.83)
45	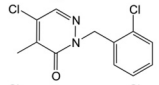	23.02 (22.28-23.79)	**>64**	**50** (46.98-53.23)	**52.97** (47.58-58.97)	36.83 (34.64-39.17)	29.24 (24.87-34.37)
42	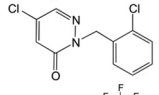	41.97 (39.43-44.67)	**>100**	**112** (107.6-116.7)	**>100**	67.96 (64.30-71.82)	63.38 (60.7-66.1)
40	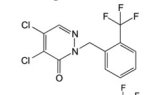	3.48 (3.13 - 3.87)	**8.69** (7.0-10.78)	5.75 (5.07-6.53)	**8.82** (7.4-10.4)	6.42 (5.2-7.92)	6.42 (5.6-7.2)
41	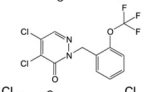	10.09 (8.96 - 11.36)	**22.76** (20.34-25.47)	**33.42** (30.88-36.16)	**29.04** (25.13-33.55)	19.62 (17.36-22.17)	16.65 (14.6-18.8)
43	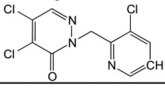	25.43 (23.63 - 27.36)	**>100**	47.15 (44.67-49.77)	**>100**	38.83 (35.94-41.96)	45.25 (41.9-48.8)

[+] *In vivo* inhibition was measured by growth inhibition of strain $lptD_{4213}$ Δ*dsbB* $dsbB_{Ptrc204}$ (CL409–10, CL416–7 and LI18–19 strains) in the presence of drugs.

tion pathway is possibly altered by a change in the rate-limiting step, which resolves the DsbA-DsbB complex, releasing reduced quinone and oxidized Cys-41–Cys-44 of DsbB. It is possible that the mutations affected this step as well by restructuring the region in the DsbA-DsbB complex in a way that the compound cannot reach Cys-44.

We showed that $DsbB_{L25P}$, $DsbB_{A29V}$, and $DsbB_{K39E}$ mutants confer *in vitro* resistance to compound 12 observed as a 5-, 50-, and 2-fold increase in the IC_{50}, respectively (Table 1, 8th column). One explanation for the finding that $DsbB_{P100S}$ and $DsbB_{F106L}$ did not show an increase of the IC_{50} value is that these mutants may have also affected the K_m value for DsbA. Even though DsbA is in excess in the conditions used *in vitro* (20 μM), this may not represent the physiological conditions, and/or the fact that DsbB is away from the membrane in the *in vitro* experiments may affect the hydrophobic environment of the membrane required to observe resistance. Future work is needed to determine whether this is the case.

Besides being found as a resistant mutant in two different selections and having a 2- and 5-fold increase in K_m for ubiquinone and menadione, respectively, a decrease in k_{cat}, and a decrease in catalytic efficiency (k_{cat}/K_m), the $DsbB_{L25P}$ mutant conferred *in vivo* resistance to all the inhibitory pyridazinones tested, and this resistance resulted in a 2–5-fold increase in the *in vivo* IC_{50} (Tables 1 and 4). Similarly, the $DsbB_{K39E}$ mutant exhibited a 2-fold increase in k_{cat} when using ubiquinone, and a 3- and 5-fold increase in K_m for ubiquinone and menadione, and it provided as well resistance to all inhibitory pyridazinones tested *in vivo*, resulting in 2–4-fold increases in the IC_{50} (Tables 1 and 4). Therefore, Leu-25 and Lys-39 may be associated with the binding of the pyridazinone ring and the phenyl ring, which is common to all the inhibitors tested. Overlapping the pyridazinone ring with the quinone ring in the DsbB structure (Fig. 3*B*), we observed that the phenyl ring is possibly oriented to the hydrophobic groove of the membrane where the methyl-butenyl group of ubiquinone-1 orients, although the pyridazinone ring may sit near Cys-44 on the periplasmic facing surface. Therefore, it is possible that Lys-39 may be responsible for binding to the pyridazinone ring and Leu-25 to the phenyl ring.

It is important to note that the DsbB mutants were selected to be at least 2-fold resistant to compound 12 under anaerobic conditions in which the abundant quinone is menaquinone (35, 36). Therefore, one explanation for the finding that some mutants conferring resistance to compound 12 anaerobically do not do so aerobically ($DsbB_{A29V}$ and $DsbB_{F106L}$) may depend on the amount and redox state of the quinone species available in the strain. It has been shown that changes in oxygen levels alter the composition and the redox states of the quinone pool (ubiquinone-8, menaquinone-8, and demethylmenaquinone-8) (36). Another possibility is that the amount of DsbA changes among growth conditions. Nevertheless, we did not observe any change in the DsbA levels of the mutants compared with wild type grown aerobically or anaerobically (data not shown). One additional observation is that these two mutants conferred *in vivo* resistance to the $lptD_{4213}$ strain to compounds that are less potent inhibitors than compound 12, with the exception of compound 38 (Table 4).

We asked whether there exist variants of DsbB enzymes that might be resistant to pyridazinones by doing a bioinformatic search among the different *E. coli*-sequenced genomes available. From the 52 DsbB protein sequences analyzed (that share 90% or greater identity), the five residues presented in this work were conserved and similar to wild type DsbB (data not shown). We also looked at the conservation of these five residues among other DsbB proteins from Gram-negative bacteria, specifically the ones that we know from our previous work are inhibited by pyridazinone-related molecules (17). The identity between DsbB proteins from *Salmonella enterica* sv. *typhimurium*, *Klebsiella pneumoniae*, *Vibrio cholerae,* and *Haemophilus influenzae* ranges from 85 to 41% when compared with *E. coli* DsbB. Among these organisms, four of the five residues were conserved overall when aligned to wild type *E. coli* DsbB, except for Lys-39. However, DsbB proteins from *Pseudomonas aeruginosa*, *Acinetobacter baumannii,* and *Francisella tularensis,* which share ~20% of identity with *E. coli* DsbB, demonstrated little or no conservation in the five residues studied. Moreover, *P. aeruginosa* DsbB1 encodes a Val-29 variant; similarly, *P. aeruginosa* DsbB2 and *A. baumannii* DsbB encode a Glu-39-resistant variant studied in this work. Nevertheless, we have shown that these proteins are still sensitive to compound 12 and related pyridazinones (17). Thus, it is possible that each enzyme may have slight differences in the structure and therefore differences in

binding to pyridazinone drugs, which is in agreement with our previous observation that the extent of inhibition changes among different pyridazinone inhibitors (17).

All mutant DsbBs were able to functionally complement the $lptD_{4213}dsbB^{-}$ strain for growth, indicating that the mutants are functional enzymes not only anaerobically but also aerobically. Similarly, the DsbB mutants were also able to complement two other $dsbB^{-}$ phenotypes. They restored motility of the *dsbB* mutant, and they also lacked β-galactosidase activity when the β-Gal^{dbs} is expressed in the strain (data not shown). However, all of the mutants obtained displayed lower catalytic efficiencies than the wild type enzyme.

Our finding that the combination of an $lptD_{4213}$ mutation and a *dsbB* null mutation are synthetically lethal leads us to suggest that any mutation or drug that decreases LptD assembly may also be synthetic lethal with the Dsb pathway (*dsbA* or *dsbB* mutants). Consequently, this finding suggests that combinations of drugs that target these two pathways can potentiate their antibiotic effect. This also suggests that inhibitors of the Dsb pathway may help to study LptD assembly by searching for mutations that confer resistance to these small molecules in order to identify additional genetic factors involved in LptD assembly (22).

The mutants studied here have a modest level of resistance (2–5-fold increase in IC_{50}) to pyridazinone molecules in *E. coli* growth. It may be that greater changes in resistance are costly to the enzyme and thus to bacterial growth. Two different spontaneous genetic selections for resistance to the pyridazinone inhibitor, anaerobic selection for growth and growth of the $lptD_{4213}$ mutant, indicate that the frequency with which resistance arises is quite low. Obtaining such mutations was only made possible by PCR mutagenesis of a plasmid-encoded *dsbB*, which artificially increased the mutation rate. Although the environment in infections may generate different conditions for selection, these initial results raise the possibility that resistance problems during infections may possibly be avoided. Our findings may provide insights to the development of more effective pyridazinone drugs that do not bind covalently and are also important for understanding the nature of resistance, which may also hold some clinical relevance. This suggests that further development of pyridazinones as potential antivirulents/antibiotics may be warranted.

Materials and methods

Bacterial strains and growth conditions

The strains and plasmids used in this study are listed in Tables 5 and 6, respectively. Standard molecular biology techniques and P1 transduction were used for the construction of strains and expression vectors (37, 38). All strains were grown in LB Miller agar or in M63 0.2% glucose liquid and agar media at 37 °C. Minimal M63 with 0.2% glucose and 40 mM fumarate solidified with 1% agarose plates were prepared for anaerobic growth experiments by placing in a Coy anaerobic chamber (85% N_2, 10% H_2, 5% CO_2) to equilibrate for several days before use. The antibiotic concentrations used were as follows: ampicillin 100 μg/ml (for plasmid copy), 25 μg/ml (for chromosomal copy), or 10 μg/ml (for $LptD_{4213}$ strain), kanamycin 40 μg/ml, tetracycline 10 μg/ml, and chloramphenicol 10 μg/ml.

dsbB mutagenesis and construction of mutant library

A mutagenic PCR of the *dsbB* gene using primers Cl13 and Cl14 was generated using the first seven mutagenic conditions of Diversify mutagenesis kit (Clontech) that on average generates 2–5.8 mutations/kb. The amplification conditions used were 94 °C (30 s) as denaturing temperature, 55 °C (30 s) as annealing, and 68 °C (30 s) as extension repeated for 25 cycles. The products were reamplified using *Taq* platinum (Thermo Fisher Scientific) to produce more of the PCR product. PCR products of all reactions were then mixed, column-purified, NcoI-SacI-digested, and ligated to a digested pDSW204 plasmid (39). 1 μl of the ligation reaction was transformed into highly competent XL1-Blue cells (Agilent Technologies). A sample of the colonies obtained after selection on ampicillin plates was collected for plasmid preparation used to confirm efficiency of ligation by PCR and digestion. Given that 9 of 10 colonies did have the expected insert, the rest of the ligation reaction (49 μl) was transformed into DH10β highly competent cells (New England Biolabs). The transformation yielded ~3,000 colonies, which were scraped up and grown overnight in M63 glucose for plasmid preparation. Plasmid preparations were frozen at −20 °C until use.

Construction of a conditionally lethal strain $lptD_{4213}$Δ*dsbB*

$lptD_{4213}$ (amino acid deletion from 330–352) mutant was constructed in *E. coli* MC1000 strain by transducing the mutation from the MC4100 strain, NR698 (22). First, the *lptD* gene was linked to a tetracycline resistance cassette (at *carB* gene, 20–25% linkage) by making a P1 lysate from the GC208 strain (40). This lysate was then used to infect the NR698 strain ($lptD_{4213}$ mutation) selecting for transductants in tetracycline plates. The $lptD_{4213}$ transductants linked to tetracycline cassette were verified by the size of the PCR product of part of *lptD* gene (1.5 kb), and the mutants have a 68-bp smaller PCR product due to the deletion of 23 amino acids using primers Cl84 and Cl85. It was also noticed that all small colonies had $lptD_{4213}$ mutation, and the regular size colonies had wild type *lptD*. Thus, this was used in later selections to distinguish between them. A P1 lysate from one verified transductant in the previous step was prepared to infect HK295 (MC1000) strain. After verifying the presence of $lptD_{4213}$ mutation in HK295, the tetracycline cassette linker was removed from the strain by P1 transduction of wild type strain and selecting on minimal M63 media, because the *carB* mutation makes the cells arginine and uracil auxotrophs on minimal media (41). The colonies that grew in minimal glucose media were again verified by PCR and sequenced to have the $lptD_{4213}$ mutation; one colony was selected for further experiments (CL337 strain).

To construct the conditionally lethal strain $lptD_{4213}$Δ*dsbB* $dsbB_{PBAD}$, first a plasmid expressing *dsbB* under the regulation of arabinose promoter (pCL67) was transformed into the $lptD_{4213}$ strain (CL337). The deletion of *dsbB* gene from HK310 strain was then P1-transduced to the $lptD_{4213}$ strain selecting on LB kanamycin plates supplemented without or with 0.2%

Table 5
Strain list used in this study

Strain	Genotype	Reference
E. coli **strains**		
HK295	MC1000 Δ*ara*714 leu^+	34
HK310	HK295 ΔdsbB (Km^r)	34
HK320	HK295 ΔdsbB	34
NR698	MC4100 $LptD_{4213}$	22
GC208	MC4100 carB::Tn10 (Tc^r)	40
JR6 (FSH94)	BL21 C43 (DE3) ΔdsbB (Km^r)	42
JR7 (FSH95)	BL21 C43 (DE3) ΔdsbB (Km^r) pWM76 ($DsbB_{C8A\ C49V}$ 6His, (Amp^r)	42
FSH69	Lemo21(DE3, Cm^r) pFL39 (6HisDsbA, Km^r)	17
CL337	HK295 $LptD_{4213}$	This study
CL380	HK295 $LptD_{4213}$ ΔdsbB (Km^r) pCL67 ($dsbB_{PBAD}$, Cm^r)	This study
CL410	HK295 $LptD_{4213}$ ΔdsbB (Km^r) pCL23 ($dsbB_{Ptrc204,\ Amp^r}$)	This study
CL417	HK295 $LptD_{4213}$ ΔdsbB (Km^r) pBOM230 ($DsbB_{L25P}$ under $Ptrc_{204}$, Amp^r)	This study
LI18	HK295 $LptD_{4213}$ ΔdsbB (Km^r) pBOM252 ($DsbB_{A29V}$ under $Ptrc_{204}$, Amp^r)	This study
LI19	HK295 $LptD_{4213}$ ΔdsbB (Km^r) pBOM253 ($DsbB_{K39E}$ under $Ptrc_{204}$, Amp^r)	This study
CL416	HK295 $LptD_{4213}$ ΔdsbB (Km^r) pBOM228 ($DsbB_{P100S}$ under $Ptrc_{204}$, Amp^r)	This study
CL409	HK295 $LptD_{4213}$ ΔdsbB (Km^r) pBOM231 ($DsbB_{F106L}$ under $Ptrc_{204}$, Amp^r)	This study
CL591	HK295ΔdsbB λatt::$DsbB_{WT}$ ($Ptrc_{204}$, Amp^r)	This study
CL592	HK295ΔdsbB λatt::$DsbB_{L25P}$ ($Ptrc_{204}$, Amp^r)	This study
CL594	HK295ΔdsbB λatt::$DsbB_{A29V}$ ($Ptrc_{204}$, Amp^r)	This study
CL595	HK295ΔdsbB λatt::$DsbB_{K39E}$ ($Ptrc_{204}$, Amp^r)	This study
CL593	HK295ΔdsbB λatt::$DsbB_{P100S}$($Ptrc_{204}$, Amp^r)	This study
CL596	HK295ΔdsbB λatt::$DsbB_{F106Y}$($Ptrc_{204}$, Amp^r)	This study
Plasmids		
pTrc99A	Expression vector, pBR322 origin, Amp^r	
pDSW204	Promoter down mutation in −35 of pTrc99A ($Ptrc_{204}$), (Amp^r)	39
pBAD45	Arabinose-inducible vector (P_{BAD}), pSC101 origin, Cm^r	45
pET28a	Expression vector, T7lac promoter, N-terminal and C-terminal His tag, thrombin cleavage site, pBR322 origin, Km^r	EMD
pWM76	pQE70-$DsbB_{C8A\ C49V}$-6His (Amp^r)	42
pFL39	pET28a-6His-DsbA cloned at NdeI-XhoI	17
pCL23	pDSW204-*dsbB* cloned at NcoI-SacI, $DsbB_{WT}$ (MV-$DsbB_{2-176}$)	This study
pCL67	pBAD45-*dsbB* cloned at EcoRI-HindIII, $DsbB_{WT}$	This study
pBOM228	pDSW204-$dsbB_{T77C}$ cloned at NcoI-SacI, $DsbB_{L25P}$	This study
pBOM252	pDSW204-$dsbB_{C89T}$ cloned at NcoI-SacI, $DsbB_{A29V}$	This study
pBOM253	pDSW204-$dsbB_{A118G}$ cloned at NcoI-SacI, $DsbB_{K39E}$	This study
pBOM230	pDSW204-$dsbB_{C301T}$ cloned at NcoI-SacI, $DsbB_{P100S}$	This study
pBOM231	pDSW204-$dsbB_{T319C}$ cloned at NcoI-SacI, $DsbB_{F106L}$	This study
pLI1	pWM76-$dsbB_{T77C}$, $DsbB_{L25P}$	This study
pLI2	pWM76-$dsbB_{C89T}$, $DsbB_{A29V}$	This study
pLI3	pWM76-$dsbB_{A118G}$, $DsbB_{K39E}$	This study
pLI4	pWM76-$dsbB_{C301T}$, $DsbB_{P100S}$	This study
pLI6	pWM76-$dsbB_{T319C}$, $DsbB_{F106L}$	This study

arabinose. Kanamycin-resistant colonies were obtained in both cases, and the transduction of the *dsbB* deletion was verified by PCR using primers Cl55–56; all checked colonies did have the correct product size (1-kb $dsbB_{WT}$ *versus* 1.6-kb *dsbB*::Km). This result indicated that the basal levels of expression from arabinose promoter were enough to complement growth in rich medium. One colony with confirmed deletion was isolated and used for further work (CL380 strain). When the *dsbB* deletion was transduced to $lptD_{4213}$ with no other copy of the *dsbB* gene, no colonies with the correct deletion of *dsbB* were obtained unless the transductants were plated on LB with 1 mM cystine; however, the transduction frequency was lower than the frequency observed in the strain with two copies of *dsbB*. The growth of CL380 strain was tested in minimal media plates. M63 glucose with 0.2% arabinose allowed growth of the CL380 strain, whereas the strain was not able to grow on M63 minimal media plates lacking arabinose. However, this strain is able to grow in liquid M63 minimal media with no arabinose under shaking conditions where oxygen may contribute to background oxidation.

Selection of DsbB mutants using $lptD_{4213}$ strain

For spontaneous resistant mutants, CL337 cells from overnight culture were washed twice with M63 minimal media, and $\sim 10^9$ cells were plated in M63 glucose media plates with 10 μM compound 12 (10-fold higher the MIC). Plates were incubated for 2 days at 37 °C. 51 colonies were purified in M63 minimal media plates to characterize them. We amplified *dsbB* (primers Cl55–56) and *dsbA* (primers Cl129–130) genes by PCR from 25 colonies and sequencing of these gave a wild type sequence. We noticed that some of the selected mutants did confer resistance to bile salts, and because these mutations had been previously studied (21), we amplified and sequenced also *bamB* (primers Cl117–118), *bamD* (primers Cl119–120), and *lptE* (primers Cl131–132). 22 of 51 colonies analyzed by PCR did have a higher size product of the *bamB* gene, and the sequence of all these indicated an insertion of IS1 element in the gene. Whole-genome sequencing was performed in three of the colonies that did not have a higher size *bamB* product. Two of these did have mutations that inactivated *bamB* (one had a stop codon insertion in amino acid 240 and the other was a deletion of amino acids 252–255).

For selection of *dsbB* mutants, the plasmid mutant library was used to transform the conditionally lethal strain, CL380 ($lptD_{4213}$Δ*dsbB* $dsbB_{PBAD}$). This strain was more sensitive to ampicillin; therefore, a lower concentration of ampicillin was used (10 μg/ml) to select for transformants containing the plasmid library. The transformation gave around 4,500 indepen-

Table 6
Primers used in this study

ID	Sequence	Restriction site
Cl6	ATGCCATAGCATTTTTATCC	
Cl8	GATTTAATCTGTATCAGG	
Cl13	CTCC**ATGGTG**TTGCGATTTTTGAACCAATG (Adds V after M)	NcoI
Cl14	CGGAGCTCTTAGCGACCGAACAGATCACGTT	SacI
Cl24	GGCGCACTCCCGTTCTGGATAATGT	
Cl25	GGTCAGGTGGGACCACCGCGCTACT	
Cl55	CTGCGTCGAGTTTACGCTTGCCCCTGTA	
Cl56	GGGATCCAGCAACAATGGCAGATGAA	
Cl84	TGAGTTCTACCTGCCATATTACTGG	
Cl85	TTATCCCAACCGTTCAGCTTCCGCT	
Cl105	GTCGTGAATTCATGTTGCGATTTTTGAACCAATG	EcoRI
Cl106	CGTAAGCTTTTAGCGACCGAACAGATCACGTT	HindIII
Cl117	AGGTGAAGGGTGGGCTGCCATTGTTGC	
Cl118	GGTTAAATAACGTGGATTTTCCTACGTTAGGGCGCCCGA	
Cl119	GTTGGGGTTTTACGGCTTTGCCGTTTAATA	
Cl120	AGCGAGCCATATTTGATGAGATCGATAGCG	
Cl129	TACTGGCTGCGACAGACGGCGA	
Cl130	CAGCAAAACTTTGAATATCCACTTATGCTGA	
Cl131	CTTTCCTGCAATAACAGAGGAT	
Cl132	GATGGCGTTACTGTACGTAAAGTGATT	
L25P-f	GCTCTGGCACCGGAACTGACG	
L25P-r	AGTAAACGCCATCAACAGC	
A29V-f	GAACTGACGGtGCTGTGGTTC	
A29V-r	CAGTGCCAGAGCAGTAAAC	
K39E-f	GATGTTACTGGAACCTTGCGTG	
K39E-r	ACATGCTGGAACCACAGC	
P100S-f	CTATCCTTCGTCGTTTGCCAC	
P100S-r	AGCTGAAGCATGGTGTGC	
F106L-f	CACCTGTGATCTTATGGTTCG	
F106-r	GCAAACGGCGAAGGATAG	
Cl225	GCAGGAGTCTATGAACACGTTTCAGTGAAACCATTTAAGAAA GTGTTCTGAGTGTAGGCTGGAGCTGCTTC	
Cl226	CAAACAAGAACACGGTTGCAAAAACCGTGCCCTTAAATATTG AATCTCTATATGGGAATTAGCCATGGTCC	
Cl230	CAAACAAGAACACGGTTGCAAAAACCGTGCCCTTAAATATTG AATCTCTATGTGTAGGCTGGAGCTGCTTC	
Cl231	GTGCACATTTTCTGAACATACATGCAGCGCG	
Cl240	CCCGAACAAGGAGTTGTGCCCGTGT	

dent colonies, which were scraped and saved in glycerol stocks. After growing the library on LB broth, cells were washed twice with M63 minimal media, and $\sim 10^8$ cells were plated on M63 glucose minimal media containing 10 μM compound 12 to select for resistant mutants. After 2 days of growth at 37 °C, colonies appeared and were purified on LB plates with no antibiotic. A PCR product of the mutagenized *dsbB* gene was amplified using primers Cl24–25 (prime only to pDSW204) to sequence.

Anaerobic selection of DsbB mutants

Purified plasmids from the mutagenized library were transformed into Δ*dsbB* cells (HK320) and plated aerobically on LB with ampicillin. The transformation yielded around 3,000 colonies, which were scraped and saved as glycerol stocks to use for further selection. The mutant library obtained in Δ*dsbB* mutant was grown aerobically in M63 0.2% glucose to an A_{600} of 0.6. Cells were washed, and $\sim 10^7$ cells were plated on M63, 0.2% glucose, 40 mM fumarate, 1% agarose plates with 2 μM compound 12. Plates were then incubated at 37 °C in a Coy anaerobic chamber (85% N_2, 10% H_2, 5% CO_2) for 3 days. The resistant colonies were purified under the same conditions and then cultured aerobically to isolate plasmids. Plasmids were transformed back into Δ*dsbB* cells, and growth of the resultant transformants was tested anaerobically under selective conditions to confirm that the plasmid carried the resistance mutation. The *dsbB* gene was then sequenced with primers Cl24-Cl25 to identify the mutations.

Using lptD$_{4213}$ strain to confirm resistance of the studied DsbB mutants

To confirm resistance of the five selected mutations, the plasmids pBOM228, -30, -31, -52, and -53 were used to transform the CL380 strain. The resultant strains were then plated on LB with 0.4% arabinose plates to select for cells cured of the plasmid with the wild type copy of *dsbB* (pCL67). Because the overexpression of *dsbB* causes cell toxicity, those cells able to grow under arabinose are most likely the cells that have lost the arabinose-inducible plasmid. Purified colonies were checked for loss of chloramphenicol resistance and were verified by PCR with primers Cl24 and Cl25 that prime only to pDSW204 but not to pBAD plasmid and with primers Cl6 and Cl8 that prime only to pBAD but not to pDSW204 plasmid. The *dsbB* mutations were confirmed by sequencing.

Growth assays of lptD$_{4213}$ dsbB mutants in the presence of various pyridazinone drugs

Strains were grown overnight in minimal M63 0.2% glucose media with 5 μM IPTG (Enzo Life Sciences Inc.) to induce the expression of *dsbB*. Overnight cultures of bacteria were diluted to an A_{600} of 0.02 in M63 0.2% glucose minimal media, and 200 μl of diluted cultures were aliquoted in 96-well plates (Thermo Fisher Scientific). Serial dilutions of the drug or DMSO were added in a volume of 2 μl (1% DMSO final concentration). The plates were covered with breathable films (VWR Scientific) and

then incubated for 19 h at 37 °C and 900 rpm in an orbital shaker (Multitron ATR). The A_{600} from at least three independent experiments was read to determine the growth, and this was used to calculate the IC_{50} values (concentration that gives 50% inhibition of growth without drug) with 95% confidence intervals using GraphPad Prism (La Jolla, CA) in the function of non-linear regression (log inhibitor *versus* response with variable slope, normalized response).

Purification of DsbB proteins and enzyme kinetics

The five mutations in DsbB were generated by site-directed mutagenesis of plasmid pWM76 using the primers listed in Table 2. Then DsbB proteins were purified as described before (42). Purified proteins were at least 90% as judged from SDS-PAGE (supplemental Fig. 1). Determination of kinetic properties and IC_{50} values was done as described before with slight changes (17). Briefly, various amounts of inhibitors were mixed with 10 nM DsbB in phosphate buffer (pH 6.5) containing 0.1% *n*-dodecyl-β-D-maltopyranoside (Affymetrix Inc.), 100 mM NaCl and ubiquinone-5 (Sigma, 1–50 μM for kinetic constants and 10 μM for inhibition assays) or menadione (Sigma, 0.5–128 μM). Reactions were started at room temperature by the addition of small amounts of highly concentrated DsbA solution to give a final concentration of 20 μM. Initial velocities of DsbB-catalyzed quinone reduction were measured at 275 nm for ubiquinone and 260 nm for menadione.

Structure-activity relationship approach of related pyridazinones

Given that a substructure analysis with pyridazinones helped us previously to identify more effective inhibitors such as compound 12 (17), we decided to explore more variations in the core of the drug to validate our understanding of the drug inhibition and to find more effective inhibitors. The molecules were designed first by substituting the chlorine atoms at positions 4 and 5 of the pyridazinone ring by other halogen atoms such as bromine and by other groups that unlike halogens could act as nucleophile (electron donor) rather than electrophile (electron acceptor), *i.e.* methyl groups. Second, we substituted the benzyl group at position 2 by different rings such as thiophene and pyridine and finally changed/added substituents in the benzyl ring at the ortho position. Molecules shown in Table 2 were synthesized by Sundia MediTech Co., Ltd. (China, purity over 95% analyzed by NMR and LC-MS). The chemical synthesis protocols are presented at the end of supplemental Information. Compound 12 was purchased from Enamine (Ukraine, purity over 95% analyzed by LC-MS).

To test inhibition, all compounds were tested in β-galactosidase assays as described previously (17). Briefly, the relative inhibitory concentration 50 (RIC_{50}) values obtained in the β-galactosidase activity assay are a measure of the inhibition of DsbB in *E. coli* expressing β-Gal^{dbs} and were used to compare the potency of the drugs. The more DsbB inhibition of a drug the more β-galactosidase activity will be observed, so the concentration that gives 50% inhibition (RIC_{50}) of the total activity observed in a Δ*dsbB* strain can be used to get the increase in potency by dividing the RIC_{50} of compound 12 (0.16 μM, 95% confidence interval 0.13–0.20 μM) between the RIC_{50} of the tested compound. Thus, drugs more effective than compound 12 will have higher ratios. The results shown in Table 3 were obtained using data of at least three independent experiments.

DsbB immunoblots

Each plasmid containing *dsbB* mutants was integrated into the chromosome of the strain HK320 by λInCh method generating strains CL591–596 (43). To determine DsbB expression levels, strains CL591 to CL596 were grown aerobically in M63 minimal media with 1 mM IPTG until log phase. The lack of IPTG makes DsbB levels undetectable when *dsbB* is under *trc*204 promoter (data not shown). Proteins were TCA-precipitated, run on reducing SDS-PAGE, and immunoblotted against anti-DsbB (44). DTT was used for reducing disulfide bonds.

Author contributions—C. L. performed lptD and substructure experiments. B. M. M. performed anaerobic selection. L. M. and C. L. performed β-gal and growth assays. L. I. and F. H. purified proteins and performed *in vitro* and mass spectrometry assays. N. Q. T. purified a protein. D. B. performed bioinformatics analysis. C. L., B. M. M., and F. H. analyzed and interpreted the data. C. L., B. M. M., D. B., and J. B. discussed the data. C. L. and J. B. wrote the paper.

Acknowledgments—We thank Su Chiang and Jinbo Lee for helpful advice on medicinal chemistry. We also thank Dan Kahne for helpful discussions and kindly providing LptD strains.

References

1. Kadokura, H., Katzen, F., and Beckwith, J. (2003) Protein disulfide bond formation in prokaryotes. *Annu. Rev. Biochem.* **72,** 111–135
2. Kadokura, H., and Beckwith, J. (2010) Mechanisms of oxidative protein folding in the bacterial cell envelope. *Antioxid. Redox Signal.* **13,** 1231–1246
3. Heras, B., Shouldice, S. R., Totsika, M., Scanlon, M. J., Schembri, M. A., and Martin, J. L. (2009) DSB proteins and bacterial pathogenicity. *Nat. Rev. Microbiol.* **7,** 215–225
4. Lasica, A. M., Wyszynska, A., Szymanek, K., Majewski, P., and Jagusztyn-Krynicka, E. K. (2010) *Campylobacter* protein oxidation influences epithelial cell invasion or intracellular survival as well as intestinal tract colonization in chickens. *J. Appl. Genet.* **51,** 383–393
5. Gonzalez, M. D., Lichtensteiger, C. A., and Vimr, E. R. (2001) Adaptation of signature-tagged mutagenesis to *Escherichia coli* K1 and the infant-rat model of invasive disease. *FEMS Microbiol. Lett.* **198,** 125–128
6. Miki, T., Okada, N., and Danbara, H. (2004) Two periplasmic bisulfide oxidoreductases, DsbA and SrgA, target outer membrane protein SpiA, a component of the *Salmonella* pathogenicity island 2 type III secretion system. *J. Biol. Chem.* **279,** 34631–34642
7. Rosadini, C. V., Wong, S. M., and Akerley, B. J. (2008) The periplasmic disulfide oxidoreductase DsbA contributes to *Haemophilus influenzae* pathogenesis. *Infect. Immun.* **76,** 1498–1508
8. Kim, S. H., Park, S. Y., Heo, Y. J., and Cho, Y. H. (2008) *Drosophila melanogaster*-based screening for multihost virulence factors of *Pseudomonas aeruginosa* PA14 and identification of a virulence-attenuating factor, HudA. *Infect. Immun.* **76,** 4152–4162
9. Totsika, M., Heras, B., Wurpel, D. J., and Schembri, M. A. (2009) Characterization of two homologous disulfide bond systems involved in virulence factor biogenesis in uropathogenic *Escherichia coli* CFT073. *J. Bacteriol.* **191,** 3901–3908
10. Himpsl, S. D., Lockatell, C. V., Hebel, J. R., Johnson, D. E., and Mobley, H. L. (2008) Identification of virulence determinants in uropathogenic *Proteus mirabilis* using signature-tagged mutagenesis. *J. Med. Microbiol.* **57,** 1068–1078
11. Straskova, A., Pavkova, I., Link, M., Forslund, A. L., Kuoppa, K., Noppa, L., Kroca, M., Fucikova, A., Klimentova, J., Krocova, Z., Forsberg, A., and

Stulik, J. (2009) Proteome analysis of an attenuated *Francisella tularensis* dsbA mutant: identification of potential dsbA substrate proteins. *J. Proteome Res.* **8,** 5336–5346
12. Bardwell, J. C., McGovern, K., and Beckwith, J. (1991) Identification of a protein required for disulfide bond formation *in vivo*. *Cell* **67,** 581–589
13. Bardwell, J. C., Lee, J. O., Jander, G., Martin, N., Belin, D., and Beckwith, J. (1993) A pathway for disulfide bond formation *in vivo*. *Proc. Natl. Acad. Sci. U.S.A.* **90,** 1038–1042
14. Bader, M., Muse, W., Ballou, D. P., Gassner, C., and Bardwell, J. C. (1999) Oxidative protein folding is driven by the electron transport system. *Cell* **98,** 217–227
15. Dutton, R. J., Boyd, D., Berkmen, M., and Beckwith, J. (2008) Bacterial species exhibit diversity in their mechanisms and capacity for protein disulfide bond formation. *Proc. Natl. Acad. Sci. U.S.A.* **105,** 11933–11938
16. Wang, X., Dutton, R. J., Beckwith, J., and Boyd, D. (2011) Membrane topology and mutational analysis of *Mycobacterium tuberculosis* VKOR, a protein involved in disulfide bond formation and a homologue of human vitamin K epoxide reductase. *Antioxid. Redox Signal.* **14,** 1413–1420
17. Landeta, C., Blazyk, J. L., Hatahet, F., Meehan, B. M., Eser, M., Myrick, A., Bronstain, L., Minami, S., Arnold, H., Ke, N., Rubin, E. J., Furie, B. C., Furie, B., Beckwith, J., Dutton, R., and Boyd, D. (2015) Compounds targeting disulfide bond forming enzyme DsbB of Gram-negative bacteria. *Nat. Chem. Biol.* **11,** 292–298
18. Ruiz, N., Chng, S.-S., Hiniker, A., Kahne, D., and Silhavy, T. J. (2010) Nonconsecutive disulfide bond formation in an essential integral outer membrane protein. *Proc. Natl. Acad. Sci. U.S.A.* **107,** 12245–12250
19. Meehan, B. M., Landeta, C., Boyd, D., and Beckwith, J. (2017) The essential cell division protein FtsN contains a critical disulfide bond in a non-essential domain. *Mol. Microbiol.* **103,** 413–422
20. Sampson, B. A., Misra, R., and Benson, S. A. (1989) Identification and characterization of a new gene of *Escherichia coli* K-12 involved in outer membrane permeability. *Genetics* **122,** 491–501
21. Eggert, U. S., Ruiz, N., Falcone, B. V., Branstrom, A. A., Goldman, R. C., Silhavy, T. J., and Kahne, D. (2001) Genetic basis for activity differences between vancomycin and glycolipid derivatives of vancomycin. *Science* **294,** 361–364
22. Ruiz, N., Falcone, B., Kahne, D., and Silhavy, T. J. (2005) Chemical conditionality: A genetic strategy to probe organelle assembly. *Cell* **121,** 307–317
23. Chng, S.-S., Xue, M., Garner, R. A., Kadokura, H., Boyd, D., Beckwith, J., and Kahne, D. (2012) Disulfide rearrangement triggered by translocon assembly controls lipopolysaccharide export. *Science* **337,** 1665–1668
24. Lee, J., Xue, M., Wzorek, J. S., Wu, T., Grabowicz, M., Gronenberg, L. S., Sutterlin, H. A., Davis, R. M., Ruiz, N., Silhavy, T. J., and Kahne, D. E. (2016) Characterization of a stalled complex on the β-barrel assembly machine. *Proc. Natl. Acad. Sci. U.S.A.* **113,** 8717–8722
25. Inaba, K., Takahashi, Y. H., Fujieda, N., Kano, K., Miyoshi, H., and Ito, K. (2004) DsbB Elicits a red-shift of bound ubiquinone during the catalysis of DsbA oxidation. *J. Biol. Chem.* **279,** 6761–6768
26. Wu, T., Malinverni, J., Ruiz, N., Kim, S., Silhavy, T. J., and Kahne, D. (2005) Identification of a multicomponent complex required for outer membrane biogenesis in *Escherichia coli*. *Cell* **121,** 235–245
27. Vuong, P., Bennion, D., Mantei, J., Frost, D., and Misra, R. (2008) Analysis of YfgL and YaeT interactions through bioinformatics, mutagenesis, and biochemistry. *J. Bacteriol.* **190,** 1507–1517
28. Tellez, R., Jr., and Misra, R. (2012) Substitutions in the BamA β-barrel domain overcome the conditional lethal phenotype of a ΔbamB ΔbamE strain of *Escherichia coli*. *J. Bacteriol.* **194,** 317–324
29. Inaba, K., Murakami, S., Nakagawa, A., Iida, H., Kinjo, M., Ito, K., and Suzuki, M. (2009) Dynamic nature of disulphide bond formation catalysts revealed by crystal structures of DsbB. *EMBO J.* **28,** 779–791
30. Rietsch, A., Belin, D., Martin, N., and Beckwith, J. (1996) An *in vivo* pathway for disulfide bond isomerization in *Escherichia coli*. *Proc. Natl. Acad. Sci. U.S.A.* **93,** 13048–13053
31. Bader, M. W., Xie, T., Yu, C. A., and Bardwell, J. C. (2000) Disulfide bonds are generated by quinone reduction. *J. Biol. Chem.* **275,** 26082–26088
32. Kobayashi, T., and Ito, K. (1999) Respiratory chain strongly oxidizes the CXXC motif of DsbB in the *Escherichia coli* disulfide bond formation pathway. *EMBO J.* **18,** 1192–1198
33. Inaba, K., Murakami, S., Suzuki, M., Nakagawa, A., Yamashita, E., Okada, K., and Ito, K. (2006) Crystal structure of the DsbB-DsbA complex reveals a mechanism of disulfide bond generation. *Cell* **127,** 789–801
34. Kadokura, H., and Beckwith, J. (2002) Four cysteines of the membrane protein DsbB act in concert to oxidize its substrate DsbA. *EMBO J.* **21,** 2354–2363
35. Newton, N. A., Cox, G. B., and Gibson, F. (1971) The function of menaquinone (vitamin K2) in *Escherichia coli* K-12. *Biochem. Biophys. Acta* **244,** 155–166
36. Shestopalov, A. I., Bogachev, A. V., Murtazina, R. A., Viryasov, M. B., and Skulachev, V. P. (1997) Aeration-dependent changes in composition of the quinone pool in *Escherichia coli*. Evidence of post-transcriptional regulation of the quinone biosynthesis. *FEBS Lett.* **404,** 272–274
37. Miller, J. H. (1992) A short course in bacterial genetics and a laboratory manual and handbook for *Escherichia coli* and related bacteria. Cold Spring Harbor Press, Cold Spring Harbor, NY
38. Sambrook, J., and Russell, D. W. (eds) (2001) *Molecular Cloning: A Laboratory Manual,* Vols. 1–3, Cold Spring Harbor Laboratory Press, Cold Spring Harbor, NY
39. Weiss, D. S., Chen, J. C., Ghigo, J. M., Boyd, D., and Beckwith, J. (1999) Localization of FtsI (PBP3) to the septal ring requires its membrane anchor, the Z ring, FtsA, FtsQ, and FtsL. *J. Bacteriol.* **181,** 508–520
40. Chimalakonda, G., Ruiz, N., Chng, S.-S., Garner, R. A., Kahne, D., and Silhavy, T. J. (2011) Lipoprotein LptE is required for the assembly of LptD by the β-barrel assembly machine in the outer membrane of *Escherichia coli*. *Proc. Natl. Acad. Sci. U.S.A.* **108,** 2492–2497
41. Gigot, D., Crabeel, M., Feller, A., Charlier, D., Lissens, W., Glansdorff, N., and Piérard, A. (1980) Patterns of polarity in the *Escherichia coli* car AB gene cluster. *J. Bacteriol.* **143,** 914–920
42. Regeimbal, J., Gleiter, S., Trumpower, B. L., Yu, C. A., Diwakar, M., Ballou, D. P., and Bardwell, J. C. (2003) Disulfide bond formation involves a quinhydrone-type charge-transfer complex. *Proc. Natl. Acad. Sci. U.S.A.* **100,** 13779–13784
43. Boyd, D., Weiss, D. S., Chen, J. C., and Beckwith, J. (2000) Towards single-copy gene expression systems making gene cloning physiologically relevant: Lambda InCh, a simple *Escherichia coli* plasmid-chromosome shuttle system. *J. Bacteriol.* **182,** 842–847
44. Kadokura, H., Bader, M., Tian, H., Bardwell, J. C., and Beckwith, J. (2000) Roles of a conserved arginine residue of DsbB in linking protein disulfide-bond-formation pathway to the respiratory chain of *Escherichia coli*. *Proc. Natl. Acad. Sci. U.S.A.* **97,** 10884–10889
45. Guzman, L. M., Belin, D., Carson, M. J., and Beckwith, J. (1995) Tight regulation, modulation, and high-level expression by vectors containing the arabinose P(BAD) promoter. *J. Bacteriol.* **177,** 4121–4130